GA–A24102

COMPREHENSIVE GYROKINETIC SIMULATION OF TOKAMAK TURBULENCE AT FINITE RELATIVE GYRORADIUS

by

R.E. WALTZ, J. CANDY, and M.N. ROSENBLUTH

SEPTEMBER 2002

DISCLAIMER

GA–A24102

COMPREHENSIVE GYROKINETIC SIMULATION OF TOKAMAK TURBULENCE AT FINITE RELATIVE GYRORADIUS

by
R.E. WALTZ, J. CANDY, and M.N. ROSENBLUTH

This is a preprint of a paper to be presented at the 19th IAEA Fusion Energy Conference, October 14–19, 2002, Lyon, France, and to be published in the *Proceedings (CD-Rom).*

Work supported in part by
U.S. Department of Energy under
Grant DE-FG03-95ER54309 and
SciDAC Plasma Microturbulence Project

GENERAL ATOMICS PROJECT 03726
SEPTEMBER 2002

Comprehensive Gyrokinetic Simulation of Tokamak Turbulence at Finite Relative Gyroradius

R.E. Waltz, J. Candy, and M.N. Rosenbluth

General Atomics, P.O. Box 85608, San Diego, California 92186-5608
email: waltz@fusion.gat.com

Abstract. A continuum global gyrokinetic code GYRO has been developed to comprehensively simulate turbulent transport in actual experimental profiles and allow direct quantitative comparisons to the experimental transport flows. GYRO not only treats the now standard ion temperature gradient (ITG) mode turbulence, but also treats trapped and passing electrons with collisions and finite beta, and all in real tokamak geometry. Most importantly the code operates at finite relative gyroradius (ρ^*) so as to treat the profile shear stabilization effects which break gyroBohm scaling. The code operates in a cyclic flux tube limit which allows only gyroBohm scaling and a noncylic radial annulus with physical profile variation. The later requires an adaptive source to maintain equilibrium profiles. Simple ITG simulations demonstrate the broken gyroBohm scaling paradigm of Garbet and Waltz [Phys. Plasmas **3**, 1898 (1996)]. Since broken gyroBohm scaling depends on the actual rotational velocity shear rates competing with mode growth rates, direct comprehensive simulations of the DIII–D ρ^*-scaled L-mode experiments are presented as a quantitative test of gyrokinetics and the paradigm.

1. Introduction

Over the course of the last three years, a nonlinear continuum global gyrokinetic code GYRO [1] has been developed at General Atomics to comprehensively simulate turbulent transport in tokamaks and allow direct quantitative comparisons to the experimental transport flows using actual experimental profiles and parameters. To arrive at this goal, GYRO not only treats the now standard ion temperature gradient (ITG) mode turbulence, but also treats trapped and passing electrons with collisions and finite beta, and all in real tokamak geometry. Most importantly the code operates on a radial grid at finite relative gyroradius $\rho^* = \rho_s/a$ so as to treat the profile shear stabilization effects which break gyroBohm scaling: $\chi \propto \chi_{gB} = \chi_{Bohm}.\rho^*$. ($\rho_s$ is the ion gyroradius and a is the outer minor radius.) ρ^* is a crucial parameter in scaling to reactors.

While GYRO is similar to the continuum gyrokinetic code GS2 [2], which effectively operates at vanishing ρ^* within a cyclic flux tube of infinitesimally small cross section and produces only gyroBohm scaled diffusion, GYRO can operate in a cyclic as well as radially noncyclic tube of finite size. The latter operation allows the addition of profile variation across a radial annulus and introduces a shearing in the mode phase velocities. It is now well established that shear in the equilibrium E×B velocity has a strong stabilizing effect on the plasma turbulence when the velocity shear rate is comparable to the maximum linear mode growth rate [3]. Shearing in the intrinsic mode phase velocities from variation in the plasma profiles (even without the E×B Doppler component) has a similar effect [3]. Apart from the E×B rotation driven by toroidal flows, the velocity shear rates from profile variation are proportional to ρ^* and the linear mode growth rates are independent of ρ^*. The competition between these rates results in the basic paradigm for broken gyroBohm scaling first explored by Garbet and Waltz [4]. The paradigm suggests a mixed power law scaling in ρ^*: $\chi \propto \chi_{gB}(1 - \rho^*/\rho^*_{crit})$. The ρ^*_{crit} for complete stabilization (as in an H–mode edge layer or internal transport barrier) is larger when far above threshold, where growth rates are larger. Thus Bohm scaling is apparent only when χ/χ_{gB} approximates a $1/\rho^*$ dependence over some limited range of ρ^*.

After describing the formulation of the GYRO code, boundary conditions and the importance of retaining sources when profiles vary, we review some results from Ref. [5] on the breaking of gyroBohm scaling by profile shearing in ITG-adiabatic electron simulations in simple s-α circular geometry. Finally we present the first comprehensive gyrokinetic simulation of DIII–D L-mode plasma slices with Bohm scaling.

2. Formulation of the Global Continuum Gyrokinetic Code GYRO

GYRO solves the standard electromagnetic nonlinear gyrokinetic equations [6] for perturbations around a given profile of shifted Maxwellian distributions in combination with Poisson and Ampere equations. Explicit 4th order time step Eulerian (continuum or Vlasov-fluid-like) methods are used. A detailed description of the equations and numerical methods is given in Ref. [1]. Real tokamak geometry is treated with local MHD equilibria (as formulated by Miller [7,8]) about nested flux surfaces labeled by the midplane minor radius r (normalized to the outer minor radius a). Turbulent transport is simulated in a radial slice of plasma about a "norm radius" at the slice center where the plasma parameters are quoted. The slice width is typically 30%–50% of the minor radius and O(100–200) ion gyroradii. Field line following co-ordinates are used and the full poloidal angle [$-\pi < \theta < \pi$] is covered. The code is spectral in the toroidal angle. Typically 10–16 toroidal n-modes are retained to span the low-k ITG and trapped electron modes. High-k ETG modes are not covered. For microturbulent transport in DIII–D, covering a 5th–15th of the torus (i.e. Δn = 5–15) is quite adequate. A key advantage of the toroidal spectral decomposition is that it efficiently scales to very low ρ^* (like ITER) without increasing the number of n-modes as Δn and n_{max} increase. However the disadvantage is that for larger radial slices, not only the number of radial grid points must increase linearly but the number of n-modes must increase to cover the low-k modes. Typically 8 energy grids, 4 trapped and 4 passing pitch angles are sufficient. Electron pitch angle collisions are included, but energy scattering and ion collisions are yet to be added. To minimize the fast electron transit time, we typically use a heaver electron with $\sqrt{m_i/m_e}$ = 20 instead of 60 which should have little effect in the low collisionality core plasma. At present only the ϕ and $A_{||}$ field perturbations are retained with ∇B drifts set to curvature drifts. This should be adequate for the low beta DIII–D plasmas and appropriate ∇B and $B_{||}$ perturbations will be added later. The code is fully parallelized using Message Passing Interface (MPI) and runs on local 18 and 46 processor clusters as well as the 3326 processor IBM-SP at NERSC. We have been able to obtain full physics runs with near linear processor scaling to 1024 processors. Runs on 256 processors with the most recent version complete in 24 hrs.

GYRO was developed in close conjunction with the cylic–flux tube code GS2 [2]. With cyclic radial boundary conditions on a radial slice without profile variation, GYRO closely reproduces GS2 linear results and the vanishing ρ^* nonlinear ITG-adiabatic electron "Cyclone Project" scans [9]. Noncyclic boundary "zero value–like" boundary conditions without profile variation produce virtually the same results. For example [5] in a standard simple ITG circular case on a grid r/a = [0.3,0.7] with q=2, s=1, α=0, R/a=3, a/L_t=3, a/L_n=1, and T_i/T_e=1 we obtain nearly identical [noncylic] (cyclic) gyroBohm normalized diffusivities $\chi/[\rho_s^2 c_s/a]$ = [3.17±0.45] (2.96±0.370), [3.18±0.51] (3.07±0.56), and [3.33±0.71] (3.36±1.29) for ρ_s/a = 0.0025, 0.0050, and 0.0075. $[\gamma_{max},\omega]$ = [0.130, –0.280] (c_s/a) at $\kappa_\theta \rho_s$ = 0.3. We obtained these "benign" boundary conditions by including damping layers at the edges of the slice to suppress the n=0 polarization shear layer, and external to that, a buffer layer to decrement the fields and set-up a well posed polarization charge equation.

When profile variation is included in the radial slice, a source must be included in the n=0 gyrokinetic equations. The code evolves perturbations or deviations from a given n=0 drifted Maxwellian which specify the input equilibrium temperature, density, toroidal velocity, and potential profiles. Without a source, the slow and long wave n=0 perturbations of the distribution function, even though O(ρ^*), cause significant changes in the effective driving gradients and shears of the input profiles. In fact with zero-value like boundary conditions imposed on the perturbations, increasing ρ^* causes the driving gradients to decrease and the gyroBohm normed diffusivity to decrease with ρ^*: a "false Bohm scaling" [5] can result. To avoid this profile gradient relaxation, we used an "adaptive source"

$$S(t,\hat{\varepsilon}) = \sum_{p=0}^{1} \int_0^t dt'/T_{eq} \; \exp\left[(t' - t)/T_{eq}\right] F_p(t',\hat{\varepsilon})$$

where $F(\hat{\varepsilon}) \equiv r^{-1}(\partial/\partial r) r\Gamma(\hat{\varepsilon})$ is the divergence of the flux surface average flow at energy $\hat{\varepsilon}$. p=0,1 denotes that only the two longest radial wave and half-wavelengths are included. After an initial transient where the turbulence builds to a quasi-stationary state, S behaves as a true source being nearly constant in time and containing only long radial wavelengths. The source does not remove slowly varying short wave "corrugations" in the n=0 total profile gradients which develop in the saturated turbulent state. Such "zonal flows" are crucial to nonlinear saturation.

3. ITG Adiabatic Electron Simulations Breaking GyroBohm Scaling in s-α Geometry

It is important to establish that the breaking of gyroBohm scaling is very dependent on profile shear rates compared to growth rates and hence on the actual profiles. Here, simple ITG adiabatic electron simulations in simple s-α circular geometry with several profiles: $[\hat{T},\hat{n}](r) = \left(1-\hat{r}^S\right)^{\alpha_{T,n}} \Big/ \left(1-\hat{r}_o^S\right)^{\alpha_{T,n}}$ with $\alpha_{T,n} = \left(1-\hat{r}_o^S/S\hat{r}_o^{(s-1)}\right)\left[aL_T^{-1}(r_o)\cdot aL_n^{-1}(r_o)\right]$ and $r_o/a = \hat{r}_o = 0.5$ $L_{T,n}^{-1} = d\ln(T,n)/dr$. Continuing with norm point $\hat{r}_o = 0.5$ parameters as specified above and profile parameter S=2 (parabolic profile), Fig. 1(a) with $a/L_T(\hat{r}_o) = 1.9$ shows gyroBohm scaling at the norm point close to the no profile "flat" case. Furthermore the diffusivities at the norm point are rather insensitive to the slice radial width if large enough. GyroBohm scaling is to be expected since (again at the norm point) the maximum growth rate is only 0.04 compared to the mode shear rate $\gamma_{shear} \equiv (r/q)\, d\,(qV_{phase}/r) = 0.013\,(\rho_s/0.005)$. All rates are in units of c_s/a. Even closer to threshold at $a/L_T(\hat{r}_o) = 1.5$ in Fig. 1(b), gyroBohm scaling persists over most of the slice. Even though the plasma is locally stable for $r/a < 0.5$, some low level "subcritical" transport persists in the stable region. Including diamagnetically driven E×B shear in these cases has almost no effect since the driving density gradient shears are just too small.

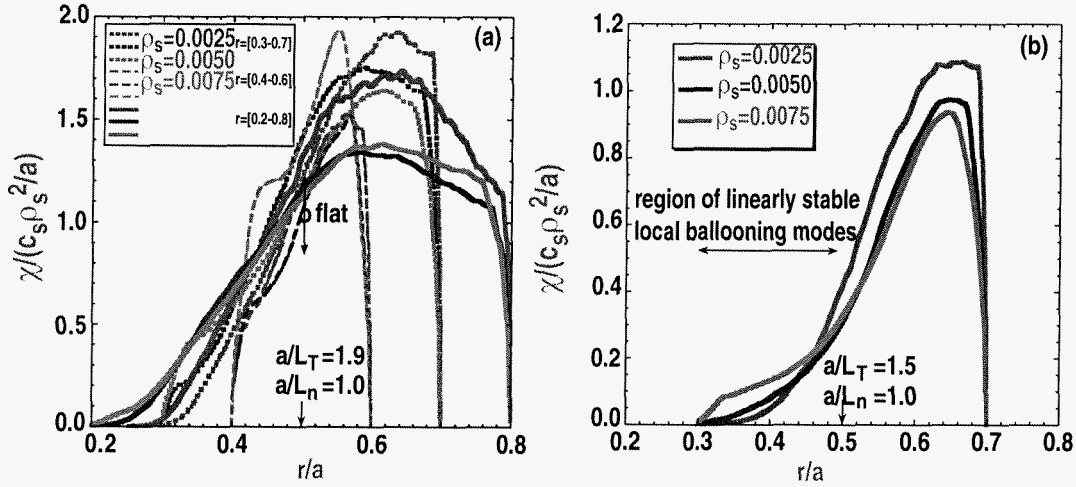

Fig. 1. Ion heat diffusivity normed to gyroBohm at the r/a=0.5 norm point versus r/a for a/L_T=1.9 (a) and 1.5 (b) with a/L_n=10, q=2, s=1, α=0, R/a=3, and T_i=T_e; ρ_s/a = 0.0025, 0.0050, and 0.0075.

To break gyroBohm scaling we retain diamagnetically driven E×B shears and go to much steeper density profiles and much smaller $\eta_i = L_n/L_T$ values (1.9–1.5 → 1.2) with $a/L_n(\hat{r}_o)$= 2.5 for $a/L_T(\hat{r}_o)$=3.0, and larger profile variation S=2,4, and 6. As shown in Fig. 2(a), Bohm scaling (and worse) is obtained at the norm point for S=4 (6) although at sufficiently small ρ*, gyroBohm scaling is recovered at the no profile variation (flat) diffusion level. The E×B γ_e (and diamagnetic temperature gradient γ_T) shear rates are inserted in the figure. At the norm point, the maximum growth rate γ_{max} = 0.09 compares to the mode shear rate γ_{shear} at S=4 and ρ* = 0.005. However at larger radii r/a=0.6, the local maximum growth rate inceases to 0.17 and the mode profile shear rate gets very small. Thus as shown in Fig. 2(b), Bohm scaling is obtained only near r/a=0.5, but at r/a=0.6 gyroBohm scaling results. About half of the broken gyroBohm scaling results from the E×B shear and the remainder from shearing in the intrinsic

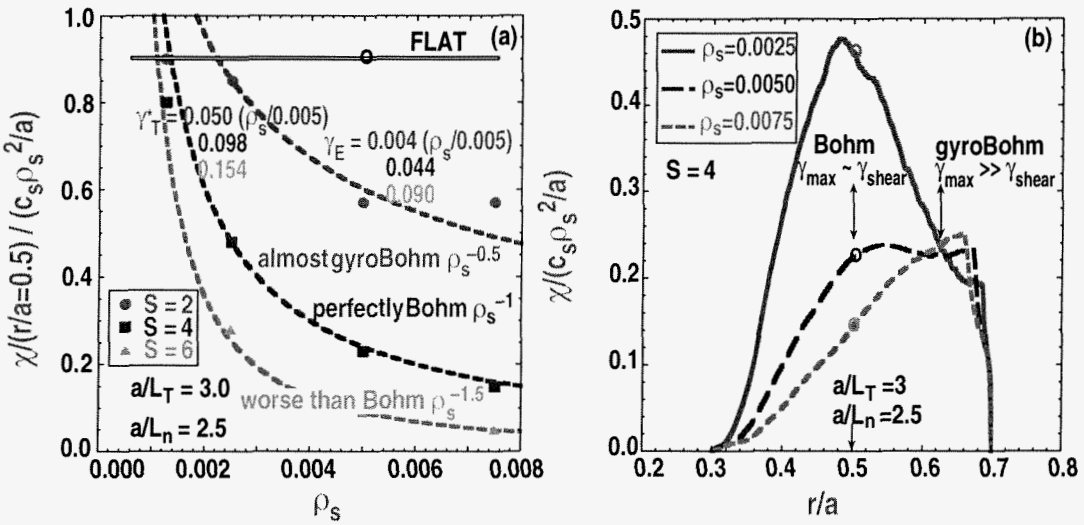

Fig. 2. Ion heat diffusivity normed to gyroBohm at the r/a=0.5 norm point versus ρ for S=2,4and 6 (a) and versus r/a in (b) for S=4 . a/L$_T$=3.0 and a/L$_n$=2.5 with other parameters as in Fig. 1.*

(non E×B) mode velocity. We have found that the decorrelation rates are independent of ρ*, but the correlation lengths (normed to a) scale as ρ* in the gyroBohm regions and $\rho^{*1/2}$ in the Bohm regions.

4. Physically Comprehensive Simulations of DIII–D Bohm Scaled L-mode Plasmas

We now use the full and comprehensive features of GYRO to simulate two ρ* scaled L-mode discharges from DIII–D: Shot 101381.2630 (1.05 T) and 101391.2790 (2.1 T) as described in Ref. [10]. Figure 3 shows the profiles of all the diffusivities about norm points at r/a=0.5 and 0.6 (electron collisions off here). Good "overlap" (i.e. same diffusivities at given r/a obtained with different norm points) indicate the validity of the slice approach. The profile of gyrokinetic linear growth rates (not shown) is extremely well matched for these discharges. We use the complete experimental profiles in real geometry explicitly including the measured E_r and V_ϕ profiles. With ITG adiabatic electron physics only, the ion diffusivities are about 1–1.5 m^2/s without E×B rotation, but essentially vanish with E×B rotation. The Kelvin-Helmholtz drive is included but negligible. With electron physics included, the diffusion levels are but about 1.7× to 2× larger than experimental values when collisions are included as shown in Table 1 for the r/a=0.6 norm. Collisions, which detrap the electrons, lower the

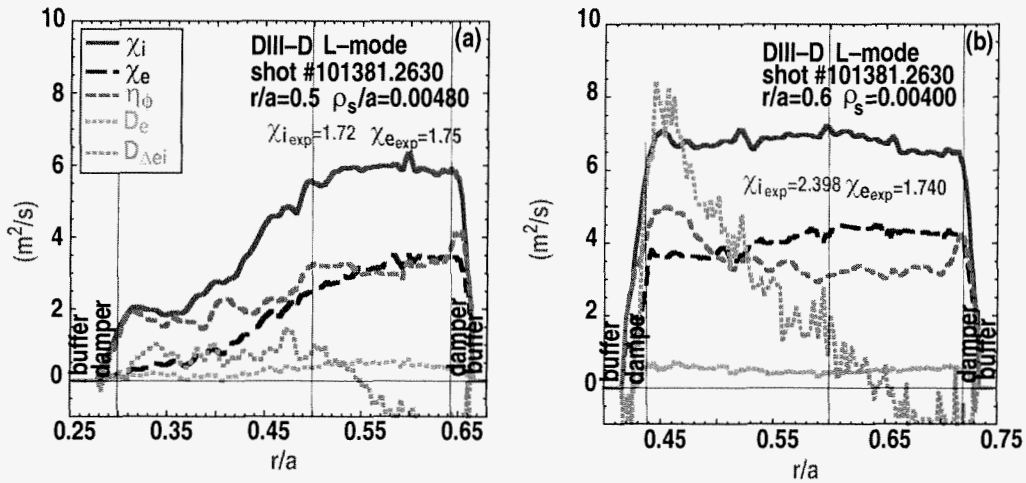

Fig. 3. Diffusivities versus r/a: χ refers to energy diffusivity (no separate convection), and η_ϕ refers to a toroidal viscosity (with separate convection) for toroidal velocity, D_e refers to electron particle diffusivity, and $D_{\Delta ei}$ is the turbulent electron-ion energy exchange rate times a^2. Electron collisions not included here.

Table 1. Analysis of DIII–D L–mode dimensionally similar discharges

	comment			ratio
B_T	exp	2.1 T	1.05 T	0.50
$\chi_{i\text{-}gB}$	exp	1.018 m^2/s	1.934 m^2/s	0.56^{-1}
ρ_s/a	exp	0.00257	0.00400	$(0.64)^{-1}$
$\chi_i/\chi_{i\text{-}gB}$	exp	2.34	1.24	0.55
$\chi_i/\chi_{i\text{-}gB}$	sim full phys	3.9	2.7	0.69
$\chi_i/\chi_{i\text{-}gB}$	sim [Fig. 3(b)] no collisions	6.0	3.6	0.60
$\chi_i/\chi_{i\text{-}gB}$	sim no E×B	5.0	4.2	0.84
$\chi_i/\chi_{i\text{-}gB}$	flux tube sim no E×B	8.1	7.7	0.96

diffusivities. Experimental error bars on the local E×B shear rate and driving temperature gradients are typically about ±30% and it is quite possible that an increased E×B shear and decreased temperature gradient within the error bars would bring the simulations into agreement with the experiments. We have not yet verified this. In any case for the ion channel, the experimental χ ratios are 0.55 which are slightly worse than Bohm (ratio of 0.64), and the full physic simulation ratio is slightly better than Bohm at 0.69. It is apparent from the Table 1 that the E×B shearing accounts for about half of the broken gyroBohm scaling even though the E×B shear rate at the large ρ^* is not markedly larger. Curiously, unlike the ITG study (in Section 3) the density correlation lengths scales as ρ^* and the correlation times as ρ^*. For the flux tube simulation with no profile variation or E×B shear, the ratio of 0.96 is nearly perfectly gyroBohm (1.0) as expected. The electron and ion channel scalings are similar although the experiment cannot accurately separate the channels in this discharge. "Magnetic flutter" transport is negligible here. Future simulations will look for gyroBohm scaling in H–modes experimental discharges.

Acknowledgment

Work supported by U.S. Department of Energy under Grant No. DE-FG03-95ER54309 and in part by the SciDAC Plasma Microturbulence Project.

References

[1] CANDY, J.M.and WALTZ, R.E., "An Eulerian Gyrokinetic-Maxwell Solver" to be published in J. Comp. Phys.
[2] DORLAND, W, ROGERS, B.N., JENKO, F., et al., Proc. 18th IAEA Fusion Energy Conference, Paper TH2/5 (2000).
[3] WALTZ, R.E. et al Phys. Plasma **2**, 2408 (1995 also **5**, 1784 (1998).
[4] GARBET, X., and WALTZ, R.E., Phys. Plasma **3**, 1898 (1996).
[5] WALTZ, R.E. CANDY, J.M., ROSENBLUTH, M.N., Phys Plasmas May 2002.
[6] FREIMAN, E.A. and CHEN, L. Phys. Fluids **25**, 502 (1982); ANTONSEN, T.M., and LANE, B., ibid **23**, 1205 (1980).
[7] MILLER, R.L. et al, Phys. Plasma **5**, 973 (1998).
[8] WALTZ, R.E. and MILLER, R.L., Phys. Plasma **6**, 4265 (1999).
[9] DIMITS, A.M. et al, Phys. Plasmas **7**, 969 (2000).
[10] MCKEE, G.R. PETTY, C.C. WALTZ, R.E. et al., Proc. 18th IAEA Fusion Energy Conference, Paper EX6/5 (2000).